Effects of Wave-Current Interactions on the Performance of Tidal Stream Turbines

Stephanie Ordonez-Sanchez[#1], Kate Porter[#2], Carwyn Frost[*1], Matthew Allmark[*2], Cameron Johnstone[#3], Tim O'Doherty[*3]

[#]*Energy Systems Research Unit, University of Strathclyde*
Glasgow, G1 1XJ, United Kingdom
[1]s.ordonez@strath.ac.uk
[2]kate.porter@strath.ac.uk
[3]cameron.johnstone@strath.ac.uk
[*] *School of Engineering, Cardiff University*
Cardiff CF24 3AA, United Kingdom
[1] frostc1@cardiff.ac.uk
[2]AllmarkMJ1@cardiff.ac.uk
[3]Odoherty@cardiff.ac.uk

Abstract—**The main objective of this paper is to analyse extreme cases of wave-current interactions on tidal stream energy converters. Experiments were undertaken in the INSEAN tow tank facility where carriage speeds of 0.5 and 1m/s were used with and without waves. The waves studied in this testing campaign had wave heights of 0.2 to 0.4m with a 2s wave period in a stationary reference frame. These wave conditions were considered extreme cases considering the use of a turbine with a rotor diameter of 0.5m. The turbine was equipped with a torque transducer, an encoder and a strain gauge to measure both the rotor torque and the forces on a single blade root. The results of the experiments showed that extreme wave-current cases can result in significant variations in power. Investigating the time histories of the blade root loading in wave-current conditions illuminated the importance of the relationships between the wave phase and blade angular position, and the number of blade rotational periods in a wave period. These affected the loading patterns and also the loading range seen by the blade, both of which have important implications for the fatigue life of the blade.**

Keywords— **Tidal Turbine, Extreme Environment, Wave-Current Interactions, Experiments.**

I. INTRODUCTION

The development of marine energy technology has increased rapidly in recent years. However, the industry has not yet reached a stage of commercial viability, and to date, only single turbine prototypes have been tested in the field ([1]). One reason for the difficulty in achieving financial viability in the industry is the complex and often extreme nature of the loading conditions seen by turbines that result from unsteadiness in the flow. The majority of projects have been deployed in areas no deeper than 50m which means that full-scale turbines operate in areas between 3-5D of water depth, assuming a turbine rotor diameter (D) between 10-16m. Depending on the site, the geometry of the turbine and type of support structure used (e.g. floating or rigid foundation) the turbine rotors will be affected partially or fully by wave-current interactions. For example, at the EMEC tidal testing site which is relatively sheltered, the penetration of waves was found to typically reach up to 1/3rd of the water column ([2]). It follows that in more energetic locations or during storm conditions the wave penetration will affect a significant proportion of the water column and turbines are likely to be affected by waves regardless of their submergence depth.

The computational study of Tatum et al. (2015) [3] indicated that the variation of bending moments on the blades due to the oscillatory motion of waves will translate into forces directly applied to small areas of the drivetrain, which will affect components such as bearings and seals. Nevalainen et al. (2015) [4] also showed numerically that the turbine shaft is highly affected by wave motion. Thus, the sinusoidal variations in wave-current velocities have the potential to reduce significantly the life of the drivetrain components and the rotor blades.

A number of experimental studies investigating the effects of wave-current interaction on turbines can be found in [5-7,9]. Barltrop et al. (2007) [5] undertook a large number of tests with a horizontal axis turbine (HAT) of 0.4m rotor diameter in a tow tank. In their work, information related to wave-current interactions on a tidal turbine in varying flow velocity, wave frequency and wave height for medium-high wave environments was presented. Their work gave a good insight and initial analysis on this matter. However, the results presented in this work were only obtained for one small fraction of the power and thrust curves and thus the effects of waves and currents are not fully visualised.

Similarly to [5], [6] carried out experiments to study wave-current interaction in a flume tank by varying the period and frequency of waves. Although the investigations completed in [6] gave a very good understanding of wave-current interactions by studying three waveforms with two different wave heights and two different wave frequencies, the mean

current velocity was similar in all of the cases, and thus it is not possible to identify the effects of current and waveform variation.

More recently, [7] undertook experimental analysis in a flume tank using a single flow speed of 0.5 m/s and a turbine of 0.5m rotor diameter. They found small differences between power and thrust coefficients when comparing the wave-current and exclusively current experiments, as previously seen in [5] and [6]. However, they undertook their analysis in a small flume tank with a blockage factor of almost 37%. This magnitude, which is related to the ratio of the swept area of the rotor to the cross sectional area of the corresponding test facility, can have significant effects on the performance of the turbines as has been studied by [8]. Galloway et al. (2014) [9] also investigated wave-current interactions on marine turbines; but in this case, the experimental campaign was only focused on a single wave-current event.

This paper aims to build on the findings of previous studies by measuring turbine torque and blade root loading under wave-current conditions over a full range of turbine rotational speeds, at two different carriage speeds and with a range of wave conditions. The tests were also conducted under the current conditions alone to enable the effects of waves to be seen more clearly through comparison of the two cases.

The focus of the experiments is on the effects of waves that represent the more severe conditions under which a turbine may have to operate. While in many locations these events will occur relatively infrequently, the impacts on turbine components may still be significant, especially with respect to their fatigue life. Ultimately, this type of loading may have important implications for the durability and also potentially the survivability of the turbine. In these tests the most severe wave case had a maximum velocity at turbine hub height equal to over 40% of the current velocity.

The focus of many of the previous studies has been on the average values of the turbine torque and thrust during wave-current conditions. In this paper the time history of the torque and blade root loads will also be analysed. In particular, the relationship between the rotational speed of the turbine compared to the wave period will be investigated, as well as the effect of the blade angular position relative to the phase of the wave. This will enable the best and worst cases for loading to be determined, and thereby inform new design and control strategies to mitigate wave loading effects.

II. Experimental Set-Up

A scaled horizontal axis turbine of 0.5m in diameter was utilised in this testing campaign. The rotor was composed of three Wortmann FX 63-37 blade profiles. The tests were carried out at the 3.5 x 9 x 220m CNR-INSEAN towing tank facility, enabling a very low blockage ratio of less than 1% to be realised. The turbine hub centre was installed 1m below still water level with the use of a steel pole, attached directly to the towing carriage. The thickness of the steel pole was chosen to prevent any significant vibrations occurring while the turbine was in operation. Figure 1 shows the turbine installed in the facility.

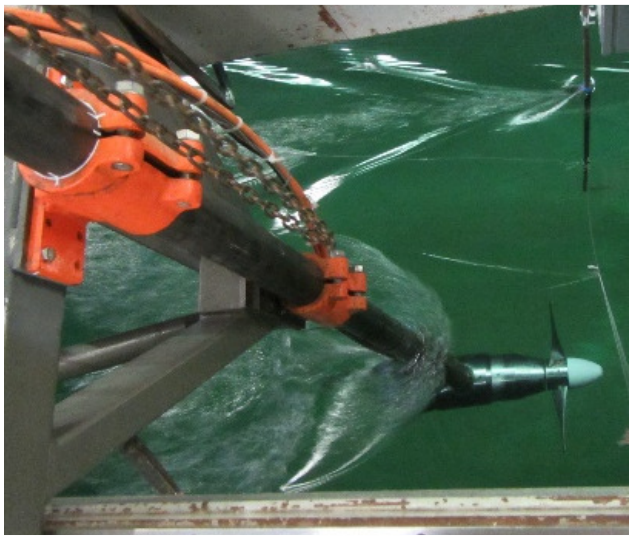

Fig. 1: Turbine set-up in the CNR-INSEAN tow tank.

TABLE I
WAVES PARAMETERS UTILISED IN THE EXPERIMENTS

Waveform	Wave height (m)	Wave Period (s)	T_a (s) (0.5m/s carriage speed)	T_a (s) (1m/s carriage speed)
WF1	0.4	2	1.72	1.51
WF2	0.3	2	1.72	1.51
WF3	0.2	2	1.72	1.51

A Bosch Rexroth AG IndraDyn T motor was employed to control the turbine by fixing either the rotor speed or torque to the desired value during each test run. The speed and position of the rotor were monitored during testing using an encoder.

The motor parameters including the torque generating current (TGC) required by the motor to set the speed or torque was logged using a National Instruments data acquisition system at a sampling frequency of 250Hz. The TGC was used to compute the rotor torque generated due to the water flowing past the blades; the details of this calculation procedure are given in Section III A.

Additionally, the turbine was equipped with a custom built strain gauging system to measure the forces at the root of one of the blades. The calibration procedure for the strain gauge is discussed in Section III B.

A wave probe to measure the accuracy of the wave height created by the wave makers was also installed on the carriage in line with the rotor head, and a Pitot tube was used to monitor the flow velocity at the height of the rotor hub.

The test programme consisted primarily of speed-controlled cases, but in one test the torque was held constant for comparison. A range of turbine rotational speeds were selected which corresponded to TSRs of 1.5-5.5, thereby encompassing the expected optimum operating point. For each turbine rotational speed the tests were conducted with and without waves at two carriage speeds of 0.5 and 1.0 m/s. Three different waves were investigated with variations of wave height from 0.2 to 0.4m and a period of 2s in a stationary frame of reference. The waves propagated towards the turbine and in the same

direction as the flow past the turbine created by moving the tow carriage. The apparent wave period, T_a, was 1.51s at a carriage speed of 1m/s and 1.72s at the 0.5 m/s carriage speed. Table I describes the waveforms used during the experiments.

To investigate the effect of the blade angular position compared to the wave phase on blade loading, two tests were conducted where the rotational period of the rotor was set equal to the apparent wave period. In the first case the upright blade position was synchronised approximately with a wave crest passing, and in the second case the upright blade was synchronised approximately with a wave trough passing. This was done by varying the rotor RPM by a small amount above or below the desired value with the waves and carriage running in order to facilitate a match with the desired phase of the wave. Once a match was achieved and the RPM reset to the correct value the test recording was begun. While this method resulted in only an approximate synchronisation, it did provide some useful initial insights into the effects on blade loading of the relationship between blade angular position and wave phase through comparison of the two cases, see discussion in Section IV G.

III. Data Processing and Calibration

A comparative analysis of the performance characteristics of the turbine is presented in this paper as C_p-TSR curves comparing the power capture under wave and no wave conditions. The power coefficient (C_p) was calculated as:

$$C_p=P/0.5\rho AV^3$$

where P is the calculated average power generated in Watts, which is equal to the rotor torque in Nm multiplied by the turbine angular velocity (Ω) in rad/s. The methodology for obtaining the rotor torque from the motor TGC is presented in Section III A. A is the swept area of the rotor in meters, and V denotes the unidirectional flow velocity (m/s), which in these tests is equal to the tow tank carriage velocity. The density of the water used to calculate C_p was 992 kg/m^3.

The average C_p is plotted against the average TSR values for each test run, where TSR denotes the ratio between the blade tip speed and the flow velocity (V):

$$TSR = \Omega r/V$$

where r represents the radius of the rotor in meters.

Similarly to the performance analysis, a comparative analysis of the blade root force under wave and no wave conditions was completed for a range of TSR magnitudes. The average blade root force measurements are plotted against TSR without non-dimensionalising the loading data. The reason behind this is that force measurements were only taken for a single blade. Thus, the thrust coefficient cannot be determined for the full rotor by simply multiplying the loads by the number of blades, due to the wave effects preventing the forces on one blade being equal to those on the other two. Nevertheless, studying the blade root forces for one blade can provide useful insights into the wave-current effects, especially when considering the structural performance and fatigue life of a turbine blade.

A. Torque Generating Current

The torque generating current is the current required by the motor to drive and hold the turbine at the selected rotational velocity (or torque). The TGC is related to torque by a torque constant, the magnitude of which is specific to the motor configuration and is supplied by the manufacturer:

$$T_{motor}=TGC*6.66$$

The magnitude of the TGC or motor torque will depend on the selected rotor speed, but also on how much torque the turbine rotor contributes due to the flow of water across the blades. If the turbine rotor produces a small positive torque then the motor torque (and TGC) will be reduced because the speed of rotation is maintained with the help of the rotor torque. If the rotor torque is very large, the motor will have to apply a torque in the opposite direction to prevent the turbine from going faster than the selected speed, indicated by a change of sign in the measured TGC.

Not all of the measured TGC will correspond directly to the rotor torque, because there will be some additional TGC required to overcome friction in the drive shaft in order to rotate the turbine. This component must be removed from the measured TGC in order to determine the amount of TGC that is directly counteracting the rotor torque input.

The motor torque required to overcome friction was determined by measuring the TGC at a number of different rotational speeds of the turbine, but without any rotor torque acting on it, i.e. in still water with the blades removed from the hub.

The results of this calibration are shown in Figure 2. A square polynomial approximation was fitted to the data. This approximation was used to determine the proportion of the measured torque during the experiments that could be attributed to the turbine rotor by subtracting the measured TGC from the TGC attributed to overcoming friction in the drive train for that rotor speed:

$$T_{rotor}=T_{friction}-T_{motor}$$

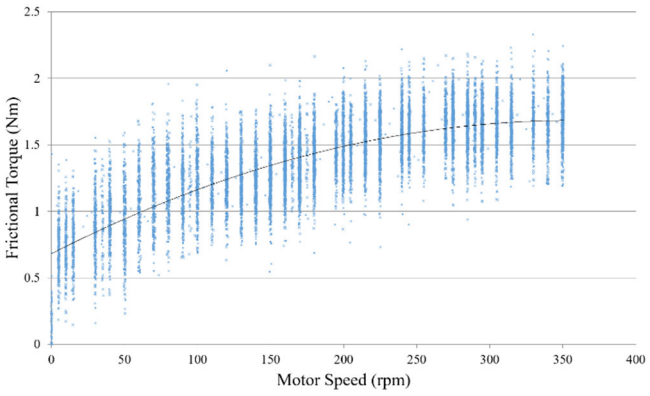

Fig. 2 Motor torque required to drive turbine hub at various rotational speeds with no rotor torque present.

Note that the frictional effects in the experiments are computed only to enable computation of the rotor torque. While frictional effects will be present at the field scale, these will not be representative in the laboratory at small scale, and where a motor is used as opposed to a generator. Consequently only the torque generated by the rotor is considered in this study, not the torque that would actually be input to the generator.

B. Blade Root Forces

The blade root forces were calibrated prior to testing by fitting several calibration weights in close proximity to the blade root connection. A linear trendline was obtained for this calibration and was used to process the raw data of the strain gauge.

An initial measurement of the blade force was obtained immediately prior to each experiment during stationary conditions; i.e. carriage at rest. This value was then subtracted from the recorded blade force value in order to convert the raw signal into informative data of the blade forces.

IV. Results and Discussion

The performance characteristics of the turbine presented in this results section include the average C_p-TSR curves for each carriage speed and the average blade root forces plotted against average TSR. The temporal variations of torque were also investigated when varying the wave height in the experiments. This information is complemented with a frequency domain analysis.

To improve understanding of the impact that the blade angular position in the water column relative to the wave phase has on loading, the time series of the blade root force measurements are considered and the magnitude of the peak fluctuations occurring in the blade root are also quantified in the following sections.

However, before these results are presented, the measurements of wave height and flow velocity are first discussed.

A. Wave and Flow Speed Measurements

The quality of the three different waveforms used in the test programme (see Table 1) was checked using a wave probe installed on the towing carriage. A summary of the mean wave heights and periods measured for the tests is depicted in Tables III and IV. The results show close agreement with the design parameters, and that the variations in these values over the sample time are small.

TABLE III
Wave Parameter Measurements at a Carriage Speed of 0.5 m/s

Cases	WF1	WF2	WF3
Mean Wave Height (m)	0.41	0.30	0.20
Mean Wave Period (s)	1.73	1.72	1.72
Standard deviation Wave Height (m)	0.02	0.01	0.01
Standard deviation Wave Period (s)	0.04	0.04	0.03

TABLE IV
Wave Parameter Measurements at a Carriage Speed of 1 m/s

Cases	WF1	WF2	WF3
Mean Wave Height (m)	0.37	0.29	0.19
Mean Wave Period (s)	1.52	1.51	1.51
Standard deviation Wave Height (m)	0.02	0.01	0.01
Standard deviation Wave Period (s)	0.04	0.04	0.08

Figures 3(a) and (b) show the typical measured water surface elevation for each of the tow speeds used in these experiments with WF1. The wave height varies by a small amount compared to the design value, likely due to limitations in the wavemaker control system which does not have active absorption capabilities. The distance from still water level to the crest is a little larger than the distance from the still water level to the trough so that the wave form contains some non-linearity. This indicates that higher order wave theory should be used to accurately model the waves. The smallest wave height gives a more linear profile with the wave crest and trough amplitudes more similar to each other. This is in agreement with the expected trend of wave non-linearity increasing with wave steepness.

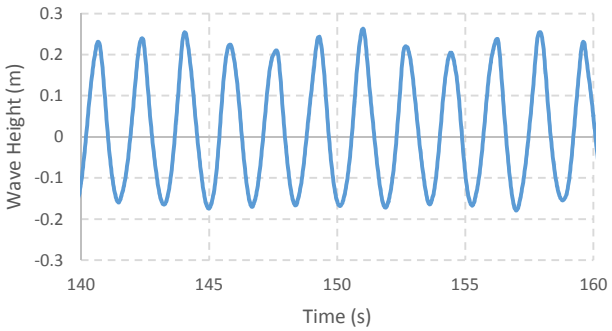

(a)

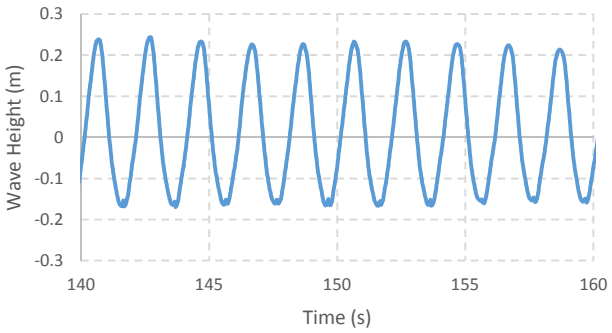

(b)

Fig. 3 Typical wave surface elevation at a) 0.5m/s and b)1 m/s with the largest of the three wave heights tested (WF1).

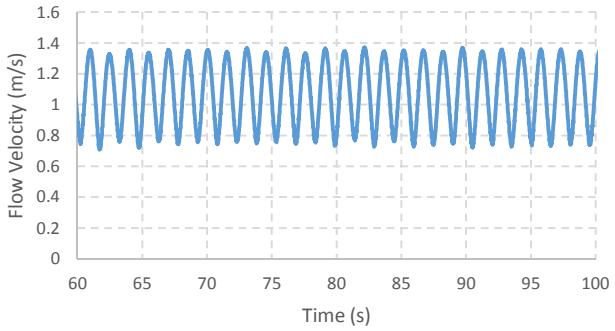

Fig. 4 Flow speed measured with a Pitot tube at 1m/s carriage speed with WF1.

The flow measurements were undertaken using a Pitot tube. The calibration method for the Pitot tube was determined to be equal to the theoretical Pitot equation with no additional correction factors. This approach gives a reasonably good agreement between the independent carriage velocity measurement and that from the Pitot tube for the steady current tests. A representative measurement of the flow velocity in waves is observed in Figure 4 using a carriage velocity of 1m/s. The measured signal is in reasonable agreement with the wave velocity computed from linear wave theory superimposed with the carriage speed.

B. Power Results

Figure 5 shows the results of the experiments undertaken at carriage speeds of 0.5 and 1m/s using WF1. In agreement with the literature, the average C_p of the turbine when working under wave-current conditions is similar to that of a turbine operating in uniform current.

The standard deviation results, shown in Figure 6, are higher by >50% compared to those found in the literature (e.g. [6]) which illustrates the effects of extreme wave-current interactions on the fluctuations in power generated by the turbine. This has important implications for the design of the power conditioning system. As the TSR increases, the standard deviation or variation in C_p increases. It can be observed that the standard deviation in C_p is higher for the 0.5m/s case where the maximum wave velocity is equal to a greater proportion of the current velocity than when operating at the 1m/s carriage speed.

As discussed in Section II the turbine was speed-controlled for the majority of the tests. In order to carry out initial investigations of using a different control technique, one torque controlled wave-current case was also investigated. The results can be observed in Figures 5(b) and 6(b) highlighted in green. The C_p value for this test (Figure 5(b)) is in agreement with the results from the speed-controlled tests. As the variations in torque are minimal under this control strategy this test is in agreement with the current only cases in terms of the standard deviation plotted in Figure 6(b). Results similar to these were also seen in [7]. This indicates that there is potential for the effects of waves on the performance of a tidal turbine to be reduced by holding the turbine torque rather than the speed at a constant value. Although, care needs to be taken not to generalise this result as only one case was tested, and the effect of using torque-control on the blade root loading also needs to be considered, see Section IV E.

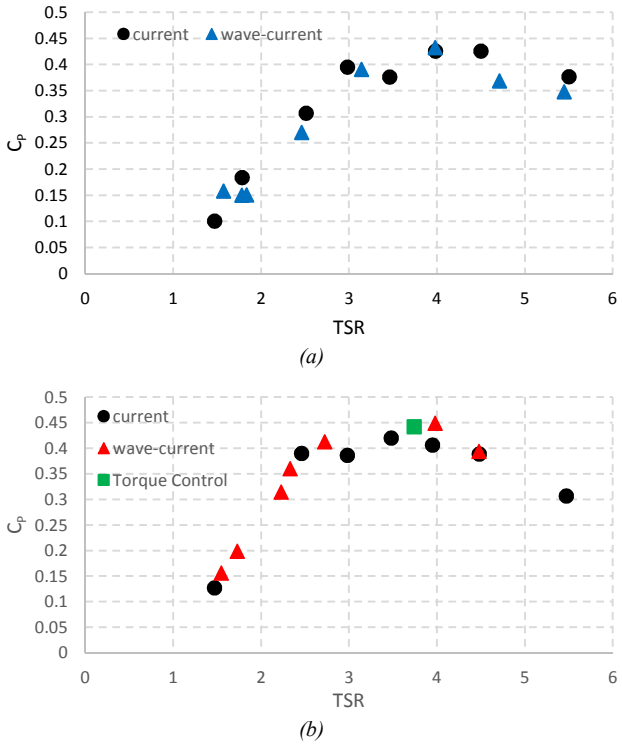

Fig. 5 Power coefficient of the turbine during extreme wave-current events (red and blue) and during current alone (black) at a) 0.5m/s and b)1 m/s.

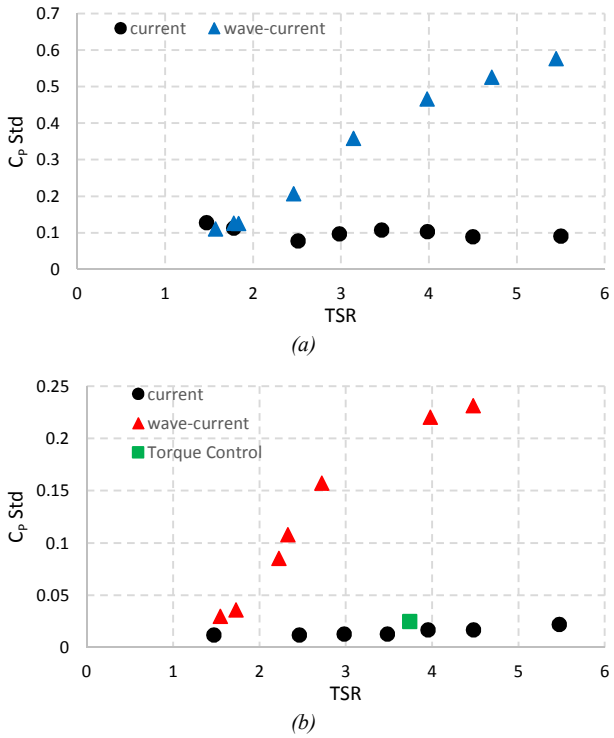

Fig. 6 Standard deviation of the power coefficient of the turbine working during extreme wave-current events (red and blue) and during current alone (black) at a) 0.5m/s and b)1 m/s.

C. Wave Height Variation – Time Domain Analysis

To investigate the effects of different wave parameters on the torque, additional experiments where the wave height was varied were undertaken at two operating TSR points at the two different carriage velocities. These are summarised in Table V.

TABLE V
CASES STUDIED WITH VARIATIONS IN WAVE HEIGHT

Cases	Flow Velocity (m/s)	TSR	Waveform
1	0.5	2.5	WF1,WF2,WF3
2	0.5	3.5	WF1,WF2,WF3
3	1	3.5	WF2,WF3

The following Table VI gives a summary of the mean power coefficient calculated for each waveform in the three test cases. The averaged C_p for the different waveforms are similar to each other in Cases 1 and 3, with a slight discrepancy of <5%. The major inconsistency is observed between the waveforms of Case 2. As expected, the variation of the C_p which in this case is given by the standard deviation decreases as the wave height decreases (from WF1-WF3) in Case 2 and Case 3, but this result is not seen for Case 1.

TABLE VI
MEAN AND STANDARD DEVIATION OF THE POWER COEFFICIENT FOR EACH WAVEFORM IN THE THREE TEST CASES

Cases	WF1	WF2	WF3
Case 1	0.27±0.21	0.26±0.17	0.27±0.20
Case 2	0.44±0.40	0.35±0.31	0.32±0.22
Case 3	-	0.43±0.15	0.44±0.11

When analysing the torque variations, it can be observed in Figure 7 that the torque range decreases by up to almost 50% as the wave height drops for a given carriage speed and TSR. It can be seen in Figures 7 (b) and (c) that doubling the carriage speed from 0.5 to 1m/s increases the torque range by 80% and 70% for WF2 and WF3 respectively. For WF1, the increase in TSR between cases 1 and 2 results in an increase in the torque range of 25%. Similarly, the torque range was 20% and 15% higher for WF2 and WF3 when using TSR=3.5 compared to TSR=2.5, respectively. The results of torque range will need to be considered when fatigue analysis is carried out on the components of the drivetrain, as observed in [4].

Comparing the torque range with the available literature is somewhat complicated as a diverse range of definitions have been used to represent this parameter. The published research that is most comparable with the tests presented in this paper can be found in [6]. In [6], a wave height of 0.28m, a wave period of 1.43s and a flow speed of around 0.7m/s were used to test a turbine with a 0.9m rotor diameter. The torque range obtained in that investigation was approximately 4.5Nm. This value is moderately higher than the one obtained in this investigation. The main reasons for this difference are the larger turbine diameter and flow velocity. Turbulence in the flow used in [6] may also result in differences between the measurements.

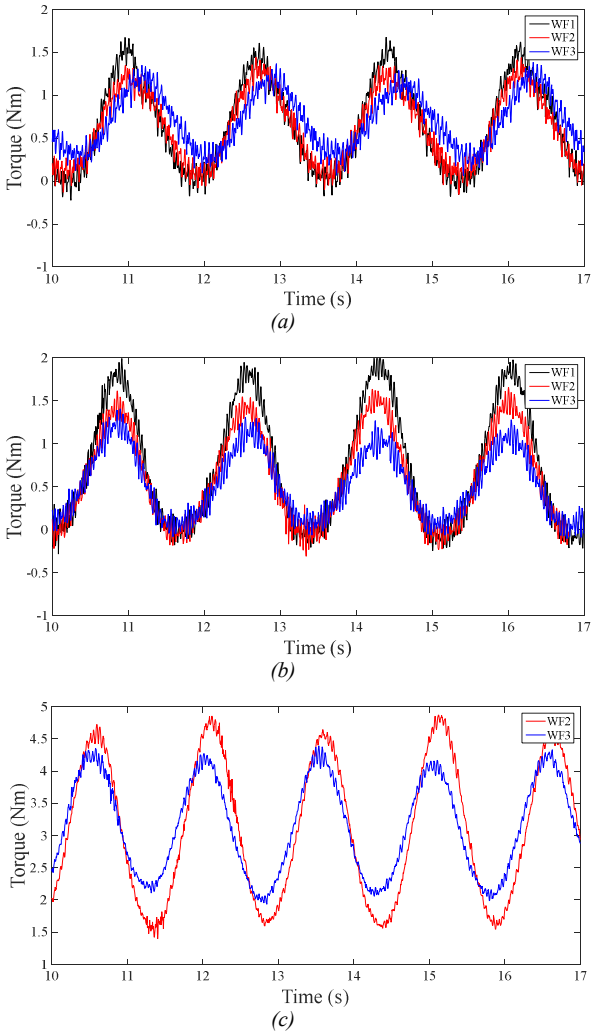

Fig. 7 Torque variation for three different wave forms when the turbine was operating at: a) 0.5m/s and TSR=2.5, b) 0.5m/s and TSR=3.5 and c) 1m/s and TSR =3.5

D. Wave Height Variation – Frequency Domain Analysis

The torque signals were investigated in the frequency domain in order to separate out the various contributions to the cyclic loading patterns in the time domain data. It can be seen in Figure 8 that the main frequency is that of the wave period, at 0.58Hz with the 0.5m/s carriage speed, and 0.66Hz at the 1m/s carriage speed. The turbine rotational frequencies of 0.8, 1.1 and 2.2Hz for Cases 1, 2 and 3 respectively provide only a small contribution to the frequency spectra. Signal noise is also evident in Figure 7 particularly around the peaks in the torque signals and this results in small contributions in the higher frequency range in Figure 8.

E. Blade Root Forces

Figure 9 shows the average blade root forces obtained at different TSRs measured on one blade at the two different carriage speeds, with and without waves. There is a reasonable match between the average blade root forces measured during the wave-current cases and during the normal operating

condition (current alone) at the 0.5m/s carriage speed. However, for the 1m/s carriage speed tests the average forces are a little higher in the wave-current cases compared to under current alone.

The tests using WF2 and WF3 are also included in Figure 9. There does not appear to be a link between the wave height and the average blade root force, as the WF2 and WF3 test results plot within the scatter of the WF1 cases.

The torque controlled test resulted in a slightly higher average force than with the speed-controlled tests, but further torque-controlled compared to speed-controlled tests would be needed to ascertain if this difference is significant or within the scatter of the data.

The range in the load signals is investigated in Figure 10 where the difference between the maximum and minimum blade root forces are plotted against the number of rotor revolutions per wave period for each test. It is observed in Figure 10 that the magnitude of the blade force oscillations is greater at the lower carriage velocity, where the maximum wave velocity corresponds to a greater proportion of the current velocity.

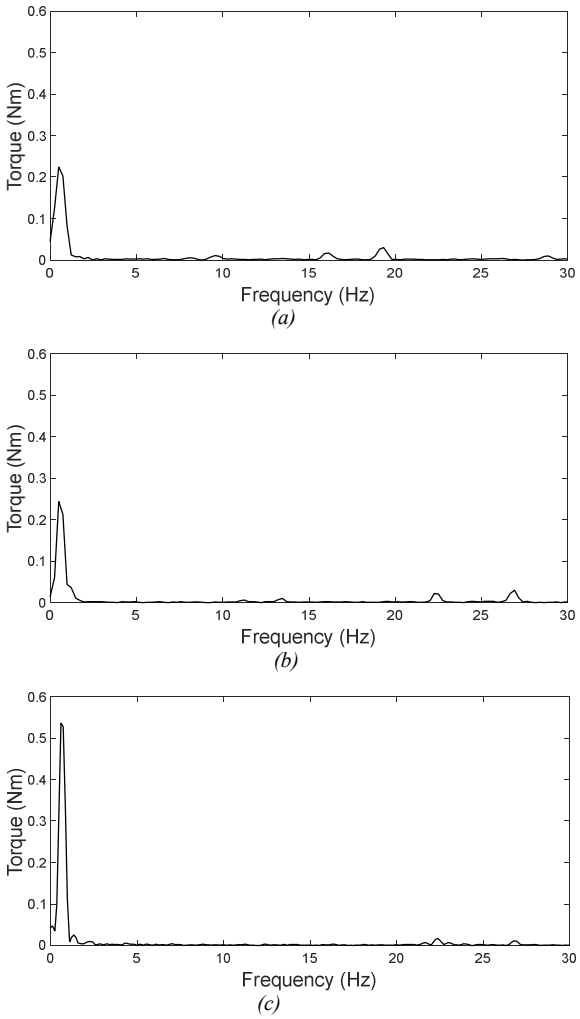

Fig. 8 Frequency domain analysis of torque variation when the turbine operates at: a) 0.5m/s with WF3 and TSR=2.5, b) 0.5m/s with WF3 and TSR=3.5 and c) 1m/s with WF3 and TSR=3.5.

The size of the oscillations decreases as the wave height decreases at a given carriage speed. This is to be expected as the fluctuations in wave-induced velocity will, therefore, also be decreasing.

The magnitude of the fluctuations also increases as the turbine rotational velocity increases compared to the wave period. This result is discussed further in Section IV F where the loading time series are analysed.

The torque-controlled test resulted in significantly larger fluctuations in the blade root forces than the speed-controlled tests under the same wave condition and carriage speed. This is an important result because this will affect the fatigue performance of the blade, as the fatigue life decreases with increasing amplitude of cyclic loading. This demonstrates the difficulty in optimising the turbine control strategy, as while speed-control may reduce the fluctuations in blade root loading, in Section IV B it was shown that the fluctuations in the power generated by the rotor were reduced through torque-control.

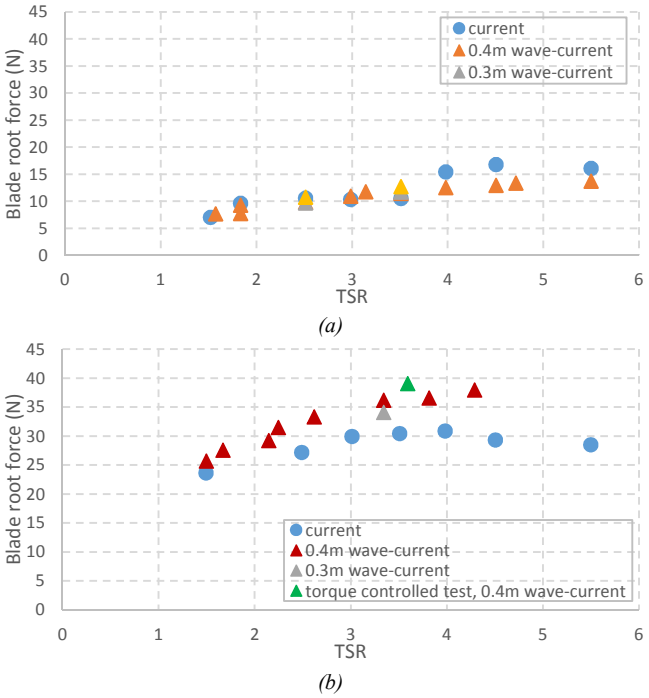

Fig. 9 Average blade forces at the root of turbine blade working during wave-current and during normal conditions (current alone) at a) 0.5m/s b) 1m/s.

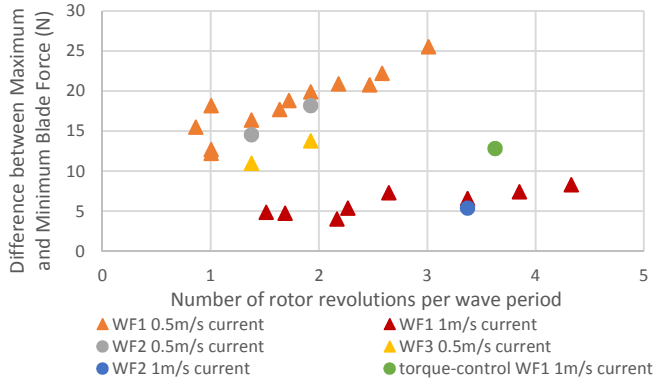

Fig. 10 Difference between maximum and minimum blade root forces versus the number of rotor revolutions per wave period.

F. *Time series of blade root forces*

More detail about the blade loading can be obtained from investigating the time series of the blade root forces. Figure 11 shows three blade root force time signals measured with a carriage velocity of 0.5m/s and WF1, but with different turbine rotational speeds. What is particularly evident is the significant difference in the pattern of the signal, depending on the rotor speed. These differences in the loading patterns are important because this may have a significant effect on the fatigue life of the blade.

The period between the peaks seen in each of the load signals corresponds to the apparent wave period. There are also repeating loading patterns occurring over a number of cycles which are marked in the Figures.

To understand the relationship between the loading patterns shown in Figure 11 and the blade rotational speed, in Figure 12 time series of the apparent wave period and the blade rotational period are plotted for each of the three cases from Figure 11. Note that the y axis has been scaled to be equal for both signals to make the comparison easier.

In Figure 12 (a) it takes approximately 7 wave periods until the two signals return to the same position relative to each other while in Figure 12 (b) this takes approximately 8 wave periods and in Figure 12 (c) approximately 13 wave periods. These numbers correspond to the number of apparent wave periods within the repeating pattern in each of the load signals marked in Figure 11. Therefore, the load patterns are a direct result of the relationship between the position of the blade relative to the wave phase.

Furthermore, in Figure 12 it can be seen that the blade rotation sometimes matches closely to a peak in the wave signal but sometimes to a minimum in the wave signal. This can explain the differences in amplitude through time in the signals in Figure 11, as the wave induced velocities in the water column are higher closer to the water surface than lower down in the water column.

The relationship between the blade angular position and the wave phase can also explain the trend in Figure 10, of increasing difference in the maximum versus minimum blade root force with increasing number of rotor revolutions per wave period. As the blade rotational period increases compared to the apparent wave period the blade will pass through more combinations of angular position compared to wave phase in one wave cycle. This will result in the amplitude of the load fluctuations increasing, as the blade is more likely to be in the upright position when both the maximum and minimum wave loadings occur within a single cycle.

Figure 13 shows a characteristic time series from a test at 1m/s carriage speed with WF1. The fluctuations are smaller than in the tests conducted at the 0.5m/s carriage speed (Figure 11) indicating that the magnitude of the wave-induced velocity compared to the current velocity has a significant influence on the loads on the turbine. The maximum horizontal wave velocity for WF1 at the depth of the turbine hub is approximately 23cm/s or 46% of the 0.5m/s carriage speed, but only 23% of the 1m/s carriage speed. This also explains the reduction in the size of the loading range when the wave height was decreased (see Figure 10).

In Figure 13 the period between the peaks in the loading signal corresponds to the apparent wave period for the test conditions (1.51s), as was the case in Figure 11. There is not a clear repeating pattern in the loading signal over several wave cycles in this case. While many of the tests conducted at the 1m/s carriage speed do not show a clear repeating pattern, the test conducted at a turbine rotational velocity of 86 RPM does, see Figure 14. As with the tests conducted at the 0.5m/s carriage speed, the length of the repeating pattern equates to the number of wave cycles until the wave period and the turbine rotational period realign, see Figure 15.

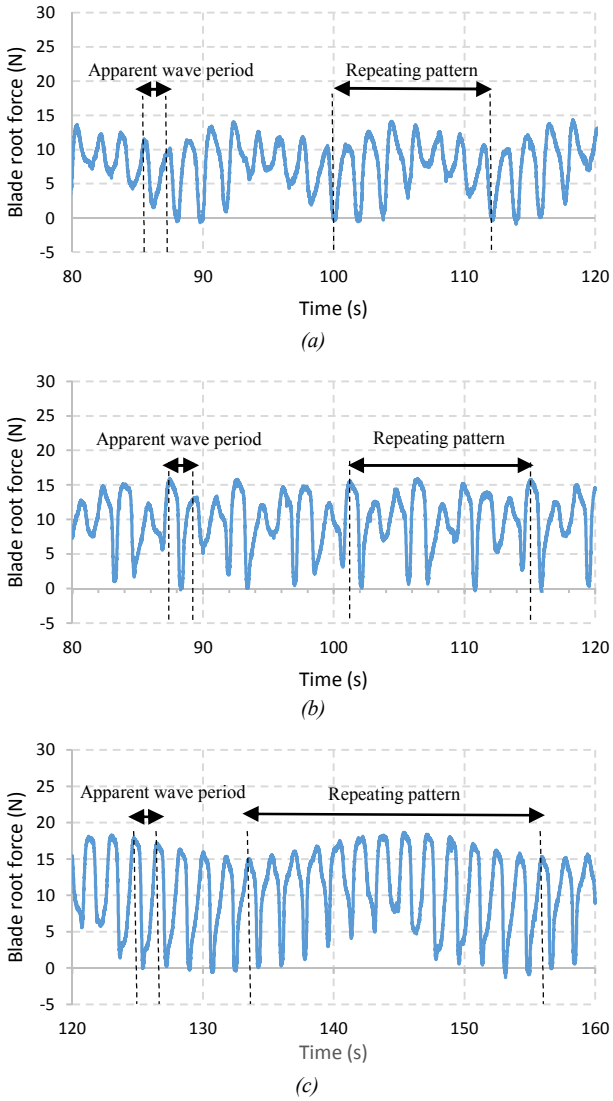

Fig. 11. Time series of the blade forces at three different rotor speeds: a) RPM=30, b) RPM=48 and c) RPM=67. Each of them measured during the experiments when the carriage was operated at 0.5m/s, WF1.

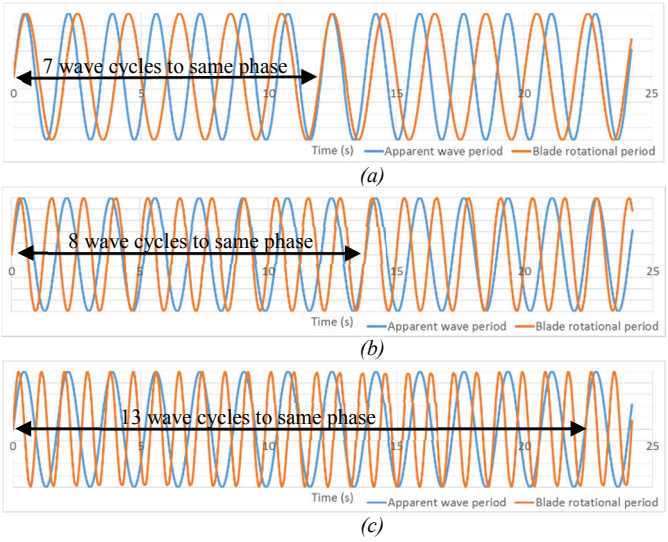

Fig. 12. Illustration of the apparent wave period and blade rotational period to show phase difference and number of cycles until the phase matches, a) RPM=30 b) RPM=48 c) RPM=67.

The lack of a repeating pattern in Figure 13 can be understood by looking more closely at the relationship between blade rotational period and wave period. The blade angular position will only truly realign with the same phase of the wave if the number of wave cycles is exactly divisible by the rotational period of the turbine. If this is not the case then the pattern will drift with time.

The amount of drift in the signals is important to consider because it is likely to affect the average load value and the range in loading seen by the blade. Where the tests have a regular pattern, or only a small amount of drift, and consequently do not cycle through as many different combinations of wave phase to blade angular position, the average blade root force and range in loading will be dependent on the blade starting position, and the length of the test time series. This may account for some of the scatter in the data in Figure 9.

G. Time series of blade forces during wave crest and trough

Two of the experiments worth further discussion are those that were carried out to evaluate the blade forces when either the wave crest or trough coincided with the instrumented blade passing the upright position. Figures 16 (a) and (b) show the time series of the blade root force signal for the two cases synchronised with the wave crest and trough respectively.

In these signals the fluctuations are more regular than those in Figure 11, as the turbine rotational speed was set equal to the apparent wave period, so that the phase difference should remain approximately constant over each cycle. However, there is a gradual change in the force patterns with time in Figure 16 due to a small discrepancy in the actual apparent wave period due to rounding, so that the turbine actually rotates by approximately 362 degrees during one wave period in these tests. During the test, the phase difference between the wave and blade angular position will drift by about 90 degrees.

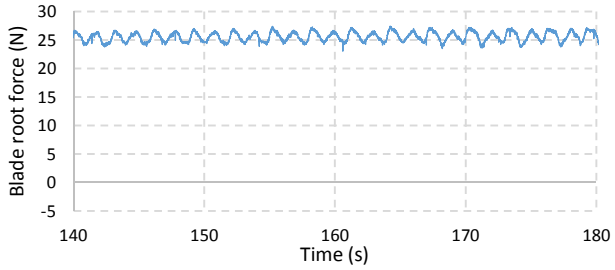

Fig. 13. Time series of the blade forces at RPM=60 measured when the with carriage speed at 1m/s, WF1. Y-axis is consistent with Figure 11 to enable comparison of the magnitude of the loads at the two different carriage speeds.

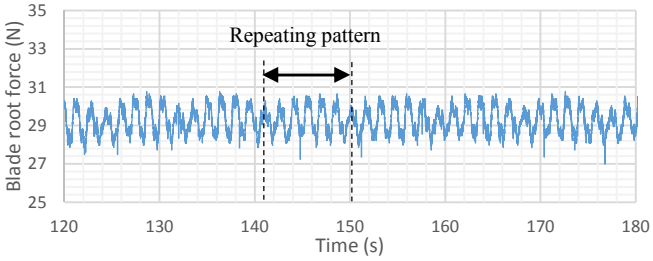

Fig. 14. Time series of blade root force at RPM=86, WF1, 1m/s carriage speed. Vertical axis zoomed to show the repeating pattern more clearly.

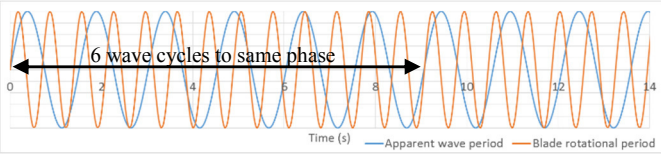

Fig. 15. Comparison of time series of apparent wave period and blade rotational period for Fig. 14: RPM=86, WF1, 1m/s carriage speed.

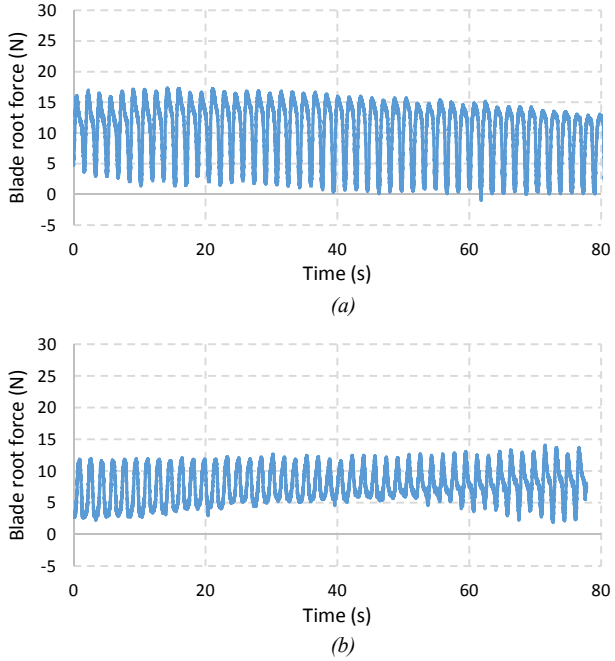

Fig. 16. Blade root forces with upright blade synchronised with: a) a wave crest and b) a wave trough at 0.5m/s carriage speed, RPM=35 with WF1.

The loading fluctuations are noticeably reduced in the test where the wave trough coincides with the upright blade, and the average loading value is also reduced (see Figures 9 and 10), as the blade is lower down in the water column when the maximum inflow velocity occurs.

It is worth considering what implications these results have at the field scale, where the turbine diameter will be between 10-20m, the current speed around 2m/s and the optimum TSR will be unchanged from the small scale, with the optimum value at around 4. These values would result in a blade rotational period of nearly 4s for a 5m blade radius, and a rotational period of approximately 8s for a 10m radius rotor blade. The rotational period of the turbine is likely in some circumstances to be of similar magnitude to the period of waves in the field, which commonly are in the range of 4-10 s or more, see [10] for data of sea conditions from a range of locations around the UK. This means that the results shown in Figure 16 may well occur in the field, and that the phase of the wave compared to the position of the blade in its rotational cycle will have a significant impact on the loading that the blade sees. Control strategies could be developed that monitor incoming waves and adjust the rotational speed of the turbine to produce the optimum position of the blades compared to the waves.

V. Conclusions

A comparative analysis of the performance characteristics of a turbine operating under extreme wave-current conditions is presented in this paper. It was found that the average power matched that under current alone, but the standard deviation was substantially higher than the information presented in the existing literature. Furthermore, the standard deviation increased with the tip speed ratio, indicating a strong dependence on the relationship between the wave period and the turbine rotational speed.

Two additional cases were tested where the wave heights were reduced, which resulted in similar power coefficients but a reduction in the range of C_P. The presence of waves with high flow velocities will increase the torque range on the rotor as will increasing the wave height in the same flow conditions.

In terms of the blade root forces, repeating patterns over several cycles in the load time histories were linked to the rotational period of the turbine compared to the apparent wave period. The severity of the oscillations depended on the position of the blade in the water column, so that the loads were larger when the blade was in the upright position due to the higher wave-induced velocities near the water surface. The range in the load also increased as the rotational speed of the turbine increased relative to the wave period. Severe oscillations of forces on turbine blades can lead to a reduced lifespan of the blades which are expensive components of tidal turbines.

It was shown that if the turbine rotational period is equal to the wave period then the average blade root force and range in the blade loading varies significantly depending on the position in which the blade is aligned with the wave. This scenario is likely to occur in the field because the rotational period of full scale turbines will be in a similar range to typical wave periods. Consequently thought should be given to possible control strategies which monitor incoming waves and position the blades more favourably relative to the phase of the wave to reduce rotor loading.

Future work will also focus on studying the effects of varying the frequency of waves on the power capture and blade root forces. Moreover, studies on this matter will include the characterisation of both parameters under extreme wave-current interactions in turbulent environments.

VI. Acknowledgments

The authors would like to thank the staff members at INSEAN for their assistance during testing. The authors would also like to acknowledge the MaRINET Transnational Access Program for funding this work.

References

[1] L. Mofor, J. Goldsmith and F. Jones, “Ocean Energy: Technology readiness, Patents, Deployment Status and Outlook.,” International Renewable Energy Agency (IRENA), 2014.

[2] J. Norris and E. Droniou, “Update on EMEC activities, resource description, and characterisation of wave-induced velocities in a tidal flow.,” in *European Wave and Tidal Energy Conference (EWTEC)* . , Porto, Portugal, 2007.

[3] S. Tatum, C. Frost, M. Allmark, D. O’Doherty, Mason-Jones, P. P. A., R. Grosvenor, C. Byrne and T. O’Doherty, “Wave–current interaction effects on tidal stream turbine performance and loading characteristics.,” *International Journal of Marine Energy.* , pp. 161-179, 2015.

[4] T. Nevalainen, C. Johnstone and A. Grant, “A sensitivity analysis on tidal stream turbine loads caused by operational, geometric design and inflow parameters,” *International Journal of Marine Energy* , vol. 16, pp. 51-64, 2016.

[5] N. Barltrop, K. Varyani, A. Grant, D. Clelland and X. Pham, “Investigation into wave-current interactions in marine current turbines,,” *Proc. IMechE Vol. 221 Part A: J. Power and Energy.,* 2007.

[6] B. Gaurier, P. Davies, A. Deuff and G. Germain, “Flume tank characterization of marine current turbine blade behaviour under current and wave loading,” *Renewable Energy, 39,* pp. 1-12, 2013.

[7] T. d. J. Henriques, S. Tedds, A. Botsari, G. Najafian, T. Hedges, C. Sutcliffe, I. Owen and R. Poole, “The effects of wave–current interaction on the performance of a model horizontal axis tidal turbine,” *International Journal of Marine Energy, 8* , pp. 17-35, 2014.

[8] C. A. Consul, R. H. J. Willden and S. C. McIntosh, “Blockage effects on the hydrodynamic performance of a marine cross-flow turbine,” *Philosophical Transactions of the Royal Society A,* 2013.

[9] P. Galloway, L. Myers and A. Bahaj, “Quantifying wave and yaw effects on a scale tidal stream turbine,” *Renewable Energy, 63,* pp. 297-307, 2014.

[10] Fugro GEOS, “Wind and wave frequency distributions for sites around the British Isles,” Offshore technology Report 2001/030, Health and Safety Executive, 2001.